

AD-A068 306

STANFORD UNIV CALIF DEPT OF GEOLOGY  
SEDIMENTATION OF NEW OCEAN CRUST: THE MID-ATLANTIC RIDGE, 37 DE--E1  
JAN 79 N S MARKS

F/G 8/7  
N00014-77-C-0390  
NL

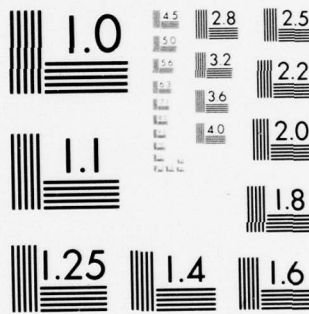
UNCLASSIFIED

| OF |

AD  
A068306



END  
DATE  
FILMED  
6-79  
DDC



MICROCOPY RESOLUTION TEST CHART  
NATIONAL BUREAU OF STANDARDS-1963-A

MIT 110  
2/71

LEVEL

1

6 SEDIMENTATION ON NEW OCEAN CRUST:  
THE MID-ATLANTIC RIDGE, 37° N

9 Master's thesis

12 72 p

DDC  
MAY 3 1979

AD A 068306

DDC FILE COPY

A THESIS  
SUBMITTED TO THE DEPARTMENT OF GEOLOGY  
AND THE COMMITTEE ON GRADUATE STUDIES  
OF STANFORD UNIVERSITY  
IN PARTIAL FULFILLMENT OF THE REQUIREMENTS  
FOR THE DEGREE OF  
MASTER OF SCIENCE

15 N00014-77-C-0390

10 By Nancy Sharman Marks

11 January, 1979

This document has been approved for public release and sale; its distribution is unlimited.

403 904

elt

ABSTRACT

→ A study of sediments from the FAMOUS area near 36°50' N latitude on the Mid-Atlantic Ridge reveals a great range of physical, chemical, and biological parameters over a small area of the sea floor.

Inside the rift valley, sediment cover patterns reflect asymmetrical spreading rates and general transport of sediments from topographic highs to low areas. A clear relationship between grain size and depth can be described by a simple linear function, with progressively finer sediments found at greater depths. The primary mechanism responsible for this distribution is thought to be gentle gravity transport of finer sediment fractions which are resuspended by bioturbation. Episodic processes, such as slumping, are believed to be less important to observed grain-size patterns than this slow but continuous process. Bottom currents are also active in the rift valley, but their primary effect is the localized formation of transient ripple and scour features.

The  $\text{CaCO}_3$  content is anomalously low in rift valley sediments, probably because of dilution of calcareous sediments by volcanic debris. The high clay content in rift valley sediments suggests that this component is mainly very fine-grained.

An examination of benthic foraminifera in the FAMOUS sediments reveals surprisingly high variability. Porcelaneous forms, particularly Spiroloculina, are especially prominent at the rift axis. A highly localized concentration of Rupertia near Fracture Zone A may possibly be related to a hydrothermal circulation system.



#### ACKNOWLEDGMENTS

I am especially grateful to Tjeerd H. van Andel for his continual guidance, support, and patience during this study. He generously made available his large collection of data from the FAMOUS area and provided helpful suggestions through every phase of this project.

I am also indebted to Libby Asbury and Pat Price of Oregon State University for the sediment analyses, Gerta Keller for help in identifying foraminifera, and Walter Brundage for providing information for the LIBEC study. I also thank David Dinter for reviewing portions of the manuscript, helping with the figures, and generally supporting this effort.

Special thanks go to James C. Ingle for much valuable advice, time, and encouragement during the foraminifera study.

This research was supported by ONR Contract N00014-77-C-0390<sup>19w</sup> with Stanford University.

TABLE OF CONTENTS

	page
LIST OF TABLES .....	vi
LIST OF ILLUSTRATIONS .....	vii
INTRODUCTION .....	1
Location and geologic setting of samples .....	1
GENERAL DISTRIBUTION OF SEDIMENTS INSIDE RIFT VALLEY .....	9
SEDIMENT TEXTURE .....	14
Relations to topography .....	15
Relations to currents inside the rift valley .....	23
Relations to rift axis .....	25
Grain size modes .....	25
CACO <sub>3</sub> CONTENT OF SEDIMENTS .....	31
BENTHIC FORAMINIFERA .....	35
CONCLUSIONS .....	50
REFERENCES .....	52
APPENDIX .....	55

LIST OF TABLES

	page
TABLE I. Correlation of sand percentage with depth of deposition. R is least squares correlation coefficient for depth versus percent sand-sized material. ....	17
TABLE II. Grain-size distribution in relation to rift axis. ..	26
TABLE III. Summary of benthic foraminifera found in samples from FAMOUS area. Samples arranged by increasing depth to the right. Numbers represent individuals counted. ....	42
TABLE IV. Relative percentages of porcelaneous, calcareous hyaline, and agglutinated foraminifera. ....	44

LIST OF ILLUSTRATIONS

	page
Figure 1. Location of samples collected by RV <u>Vema</u> in eastern North Atlantic, showing relation to FAMOUS area (small box in center). . . . .	2
Figure 2. Location of samples collected by RV <u>Knorr</u> in FAMOUS area, showing <u>Alvin</u> dive areas (dotted boxes). (From Heirtzler and van Andel, 1977.) FZ: fracture zone. . . . .	4
Figure 3. Inner rift valley topography with <u>Alvin</u> sediment sample stations marked by large dots. Dashed line represents inferred rift axis. (From Bryan and Moore, 1977.) Bathymetric contours (after Ballard and van Andel, 1977b) in meters. . . . .	7
Figure 4. General pattern of sediment cover in the inner rift valley (in percent of area per photo), based on LIBEC photo coverage. . . . .	10
Figure 5. Relation of grain size to topography in FAMOUS area, showing linear decrease in coarse fraction (>63 microns) with increasing depth. . . . .	18
Figure 6. Distribution of sand modes A through E on inner rift valley floor. Contours mark the percent of the sand fraction represented by each mode. Dashed line shows position of rift axis. . . . .	28
Figure 7. Relation of CaCO <sub>3</sub> content to depth. Note anomalously low values for inner rift valley sediments (R), when compared to other FAMOUS area samples (X). . . . .	32
Figure 8. Position of rift valley samples used in benthic foraminifera study. Field numbers are: 1)529-2/3, 2)519-1, 3)529-4, 4)529-5, 5)518-1, 6)526-4. . . . .	37
Figure 9. Position of samples associated with Fracture Zones A and B, used in foraminifera study. . . . .	39
Figure 10. Top: Distribution of porcelaneous foraminifera across rift axis. Vertical axis shows percent porcelaneous individuals in the benthic assemblage. Horizontal: sample position along traverse of Figure 8. Bottom: Distribution of <u>Spiroloculina</u> across rift axis. Vertical axis shows percent of this genus in the porcelaneous assemblage. . . . .	46

## INTRODUCTION

Project FAMOUS was an intensive study of the axial area of the Mid-Atlantic Ridge between 36°30' and 37° N latitudes (Heirtzler and van Andel, 1977). The study culminated in 1974 with a series of manned submersible dives in the inner rift valley, using the highly sophisticated DSRV Alvin (Ballard and van Ardel, 1977a). By utilizing a variety of newly-developed navigational, bathymetric, photographic, and sampling techniques, Project FAMOUS achieved a previously-unknown degree of resolution of deep-sea data. One of the benefits was the first opportunity to study on a fine scale the local and regional sedimentary environments associated with a mid-ocean rift. This study, based on analysis of all available samples from the region, is aimed at understanding the details of sediment distribution and sedimentation processes on new oceanic crust in the FAMOUS area.

Location and geologic setting of samples

Sediments sampled at three different scales were available. Over the region surrounding the Mid-Atlantic Ridge between 25° and 45° N, the RV Vema collected over forty samples (Fig. 1). The area includes several thousand kilometers of the African-North American plate boundary, which trends north-northeast and is offset by numerous east-west trending fracture zones.

The FAMOUS area, located about 400 km southwest of the Azores, was sampled by the RV Knorr in 1973 in the general vicinity of Fracture Zones A and B (Fig. 2). This portion of the Mid-Atlantic Ridge axis is characterized by a well-developed rift valley-rift

Figure 1. Location of samples collected by RV Vema in eastern North Atlantic, showing relation to FAMOUS area (small box in center).

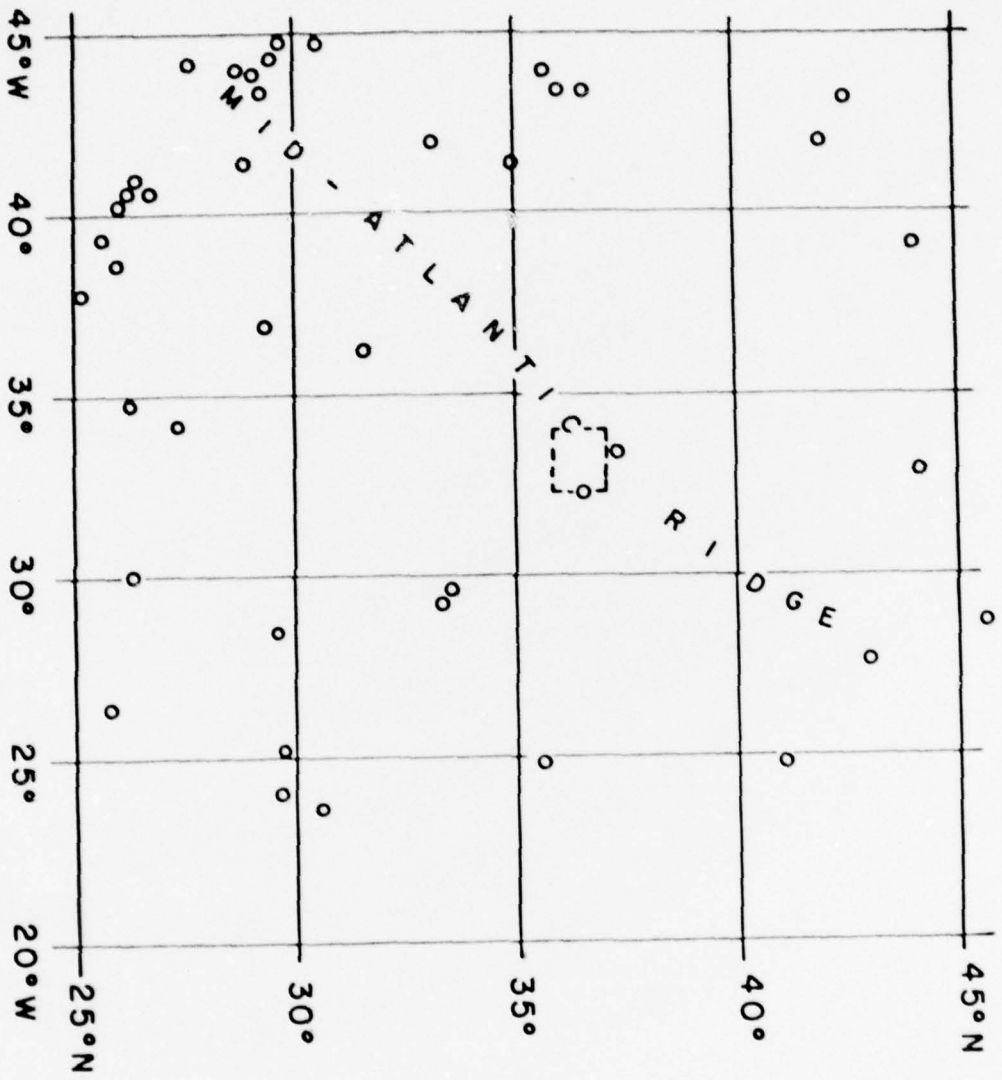
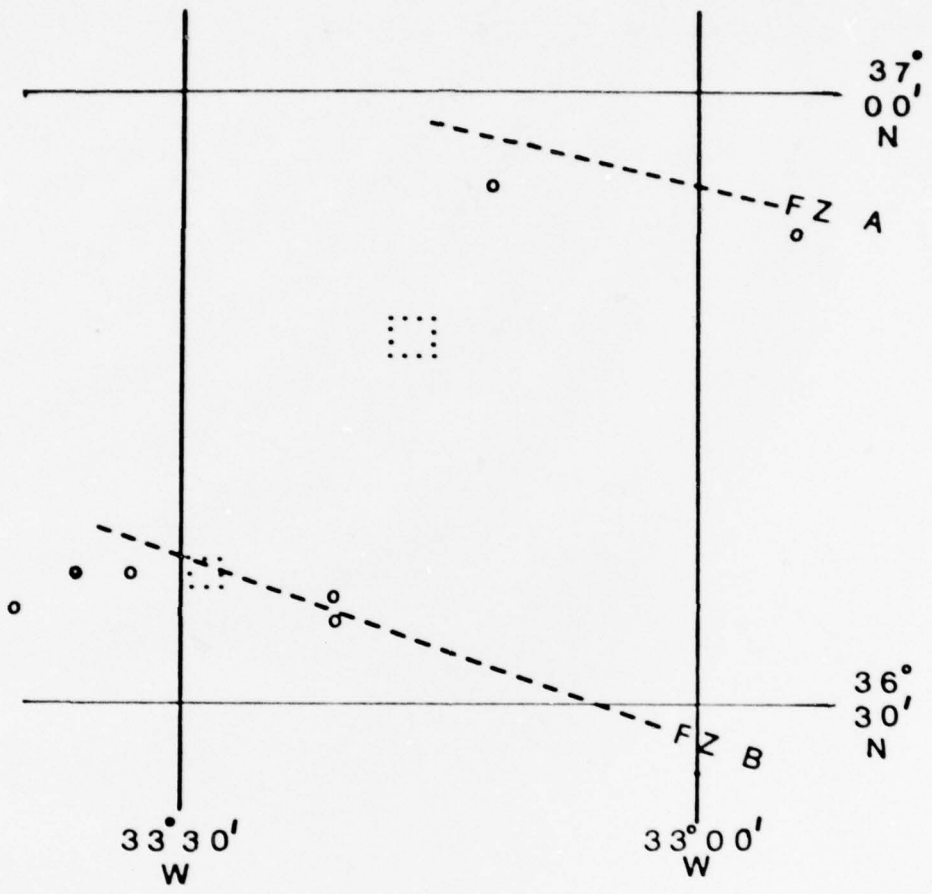


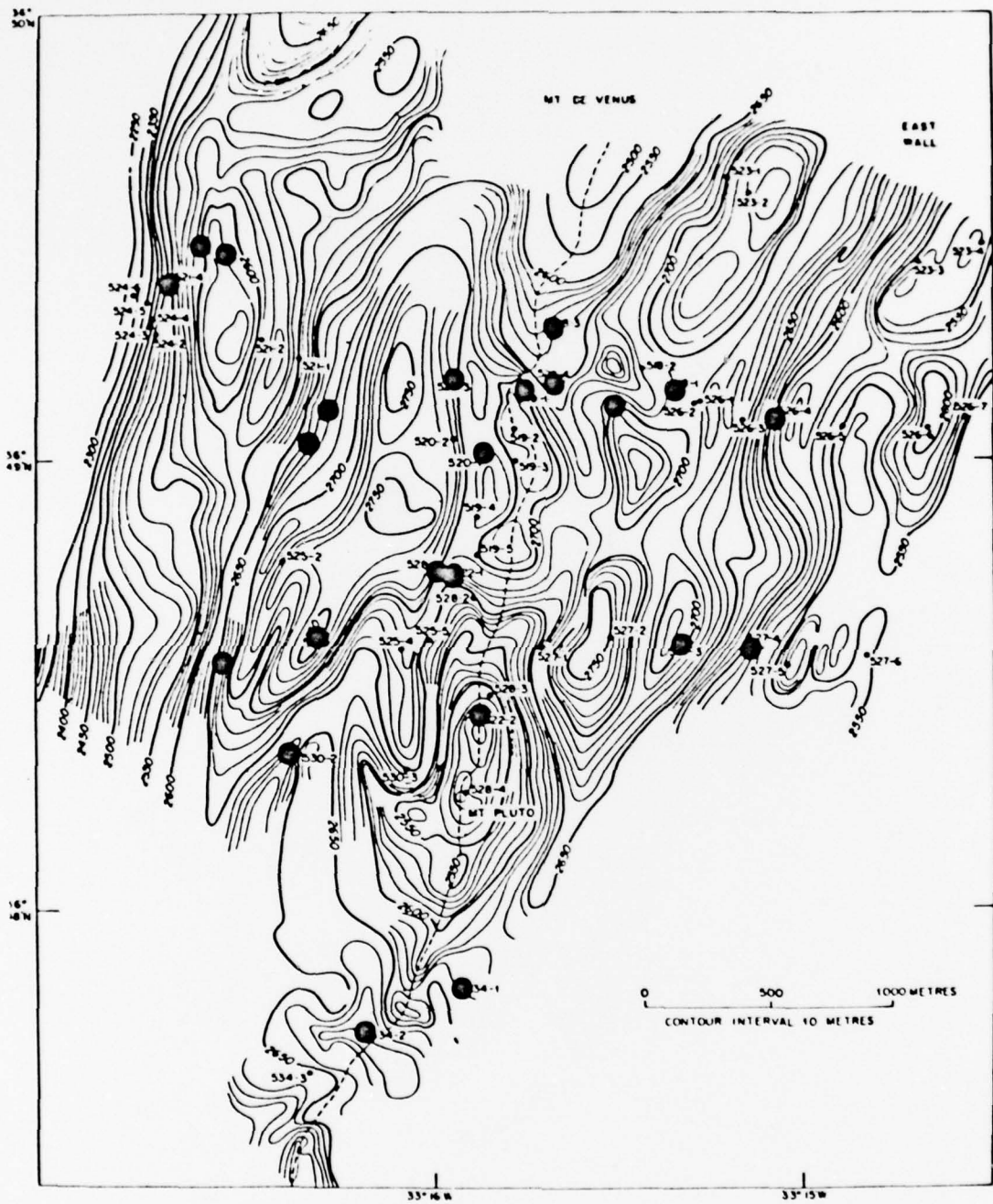
Figure 2. Location of samples collected by RV Knorr in FAMOUS area, showing Alvin dive areas (dotted boxes). (From Heirtzler and van Andel, 1977.) FZ: fracture zone.



mountain system which is offset by short (~20 km) fracture zones which are not quite orthogonal to the spreading axis (Macdonald et al., 1975). The ridge rises 1000 m above the surrounding sea floor and contains distinct provinces of varied and rugged terrain.

A small segment of the inner rift valley around 36°50' N lat. was investigated by the submersible Alvin, collecting samples from about twenty-five acoustically-positioned stations (Fig. 3). Volcanic activity and tectonic processes are reflected in the complex morphology of the inner valley (Ballard and van Andel, 1977b). The inner floor is about 2 km wide and asymmetric, with its west wall considerably steeper than the east wall (Fig. 3). Major topographic features comprise a central volcanic high, flanking marginal depressions, marginal highs, and the valley walls (Macdonald et al., 1975). Sediments are thin (up to a few meters) throughout the inner rift valley, and around the volcanic axis much of the new crust is totally exposed.

Figure 3. Inner rift valley topography with Alvin sediment sample stations marked by large dots. Dashed line represents inferred rift axis. (From Bryan and Moore, 1977.) Bathymetric contours (after Ballard and van Andel, 1977b) in meters.



## GENERAL DISTRIBUTION OF SEDIMENTS INSIDE THE RIFT VALLEY

A detailed map of sediment cover inside the rift valley was constructed in order to study relationships to physical and tectonic parameters.

The data for the map come from about 5000 bottom photographs taken by the U.S. Navy's LIBEC (Light BEhind Camera) system (see Brundage and Cherkis, 1975). The surface-towed unit includes a 70 mm camera with a seawater focal length of 40.4 mm. With distance off the bottom averaging 10-15 m, each photograph covers an area approximately 22 m across. Coverage along a given track is continuous, with successive photographs overlapping.

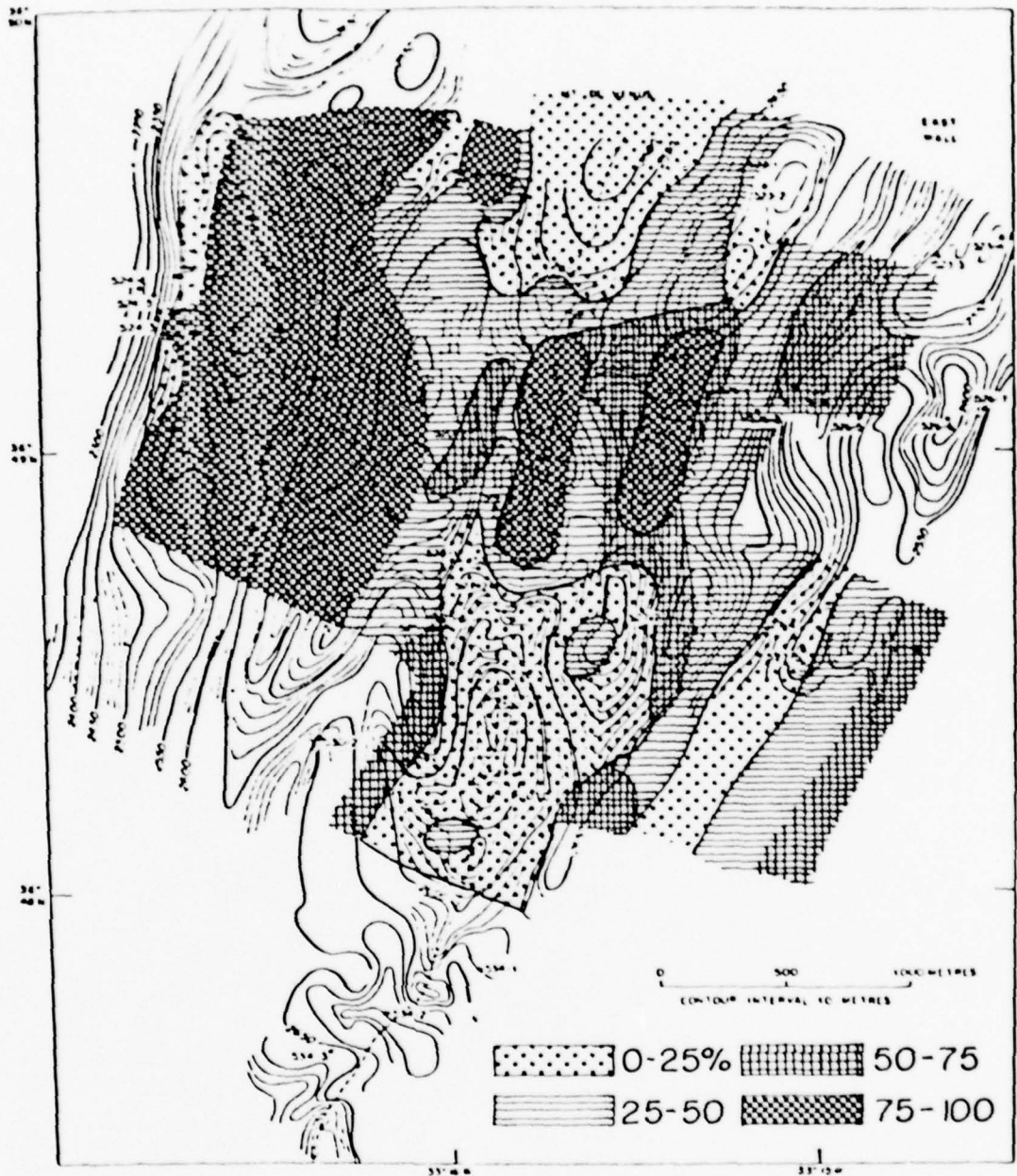
For each photograph, the percentage of the area covered by sediment was determined by point-counting, using a variable grid, depending on the coarseness of sediment distribution patterns. After about 500 photographs were analyzed in this manner, it was sometimes possible to estimate sediment cover directly with frequent checks by point-counting.

The coverage data were plotted along camera tracks and then contoured to produce a map of sediment cover for the inner rift valley between  $36^{\circ}48'$  N and  $36^{\circ}50'$  N (Fig. 4).

The map has several limitations:

- 1) Photographs were frequently of poor quality, especially along some of the earlier tracks, which made it difficult or impossible to estimate sediment cover. Nevertheless, more than 3700 data points within this small area (about  $9 \text{ km}^2$ ) are of satisfactory quality.

Figure 4. General pattern of sediment cover in the inner rift valley  
(in percent of area per photo), based on LIBEC photo coverage.



2) It is difficult to evaluate the accuracy of the method used to estimate the percentage of sediment cover. The estimates, however, are consistent, having all been made by the same person. Thus, there is a high degree of confidence in relative percentages, which are the most useful for this study.

3) Data on sediment thickness are sparse, but appear to vary from zero to a few meters within the valley. For thin sediments on irregular basalt terrain, however, the amount of coverage is a fairly good reflection of thickness.

Since the age of the terrain increases laterally away from the spreading axis, a sediment cover of increasing continuity and thickness must be expected. Such a pattern is indeed observed (Fig. 4) and, corresponding to a marked asymmetry in spreading rate (1.0 cm/yr west and 1.35 cm/yr east; Ramberg and van Andel, 1977), the most continuous cover occurs at the foot of the west wall on oldest crust.

The newly extruded oceanic basalt, nearly entirely in the form of pillow basalts, has a pronounced microrelief on several scales, ranging from a few hundred meters for individual volcanoes to several meters for portions of a flow on the scale of the individual LIBEC photos. Thus, complete blanketing with sediments will be achieved on this scale only with several meters of sediment. A pelagic sedimentation rate of about  $2.9 \text{ cm}/10^3 \text{ yr}$  has been inferred for an undisturbed core in the rift valley (Nozaki et al., 1977), a value in good agreement with a general estimate for the Neogene of  $1-3 \text{ cm}/10^3 \text{ yr}$  (Berger and von Rad, 1972). This would imply an undisturbed thickness of about 3.5 m at the eastern margin of the rift valley and 5.1 m

at the base of the west wall, using crustal ages from Ballard and van Andel (1977b), or a nearly complete cover of normal pillow basalt microrelief.

Even on or near the rift axis, the sediment cover is, at times, complete on the scale of one or more LIBEC photos, implying a thickness of several meters. This is the result of erosion and redeposition.

In general, sediment is transported from relative topographic highs to surrounding low areas. On the scale of the entire rift valley, the results of transport are deviations from the simple age relations discussed above. These can best be seen along the central volcanic zone (Fig. 4). Two prominent areas of negligible sediment cover correspond to Mt. Venus and Mt. Pluto, two volcanic highs. The low-lying region between them, which is approximately the same age, is much more heavily sedimented as a result of downhill transport. The mechanisms controlling sediment redistribution are discussed in more detail below.

The anomalously sparse sediment zone along the west wall mostly represents talus slopes (for this study, talus was not included with sediments) where talus accumulation rates exceed those of pelagic sediment. They are nearly ubiquitous along the steep west wall, but less common along the more gently sloping east wall of the rift valley.

## SEDIMENT TEXTURE

Sediment analyses were carried out on all samples shown on Figs. 1-3 at the sediment laboratory of the School of Oceanography, Oregon State University. After splitting the samples into sand ( $>63$  microns), silt ( $63-4$  microns), and clay ( $<4$  microns) fractions, grain-size distributions were determined with the automated system described by Thiede et al. (1976). Calcium carbonate content was determined with a LECO carbon analyser.

The sediments are calcareous fossiliferous oozes. The finer fractions appear to be composed largely of coccoliths and small planktonic foraminifera, as well as fragments of larger individuals. The sand fraction was examined under a microscope and found to comprise the following three major components:

1) Biogenic--approximately 90-99% of each sample consists of planktonic foraminifera. Common species identified are Globigerina bulloides, G. rubra, Globigerinoides sacculifer, Globorotalia hirsuta, G. inflata, G. scitula, G. truncatulinoides, and Orbulina universa, in addition to unidentified species of Globoquadrina, Hastigerina, and Neogloboquadrina. Less than 1% of each foraminiferal assemblage is composed of benthic species, which are generally slightly larger than most of the planktonic individuals. Other biogenic components include small, but varying, percentages of radiolaria, sponge spicules, pteropods, ostracods, and tiny mollusca.

In some areas of the inner rift valley, dense patches of pteropod debris are observed to form fluffy, nearly neutrally-buoyant deposits which appear to "float" above the other sediments. These deposits are not seen in the cores because they tend to disperse so easily when disturbed. The pteropod shells are commonly stained strongly with Mn-hydroxides and will, in part, be much older than the underlying sediments, because it is likely that the rain of pelagic material easily passes through the pteropod layer. The deposits appear to be exceptions to normal grain-size-related processes of sedimentation, mixing, and transport.

2) Volcanic--close to the rift axis, volcanic debris is very common, comprising a few percent of some samples. Dark pumice fragments up to 0.5 cm across, and clear to smoky glass shards, perhaps spalled off cooling basalt crust, are included in the sand fraction.

3) Hydrothermal alteration products--a purplish manganese stain frequently coats sediment components, and is especially evident on larger biogenic grains and volcanic ash close to the rift axis. The pumice fragments often take on a bright yellow to red tint as a result of these alterations.

#### Relations to topography

The grain size of the sediments can be expected to be a function of the size of the various components available, modified by selective transport after reaching the sea floor, and by dissolution of carbonate. A clear indication of the relation between size and area of deposition can be seen in the dependence of the sand-size fraction

on depth in the three regions of study, the inner rift valley, the general FAMOUS area, and the eastern North Atlantic.

It is obvious from Table I that, within the inner rift valley, with samples ranging in depth from 2526 m to 2750 m, there is no correlation between percent sand and depth ( $R = -0.04$ ). Direct observations from Alvin, however, indicate ongoing small-scale sediment transport by several mechanisms, as discussed below. Average grain-size values for this area fit very well with regional trends observed below.

In the FAMOUS area as a whole, within a depth range of 1967 m to 3165 m, the sand fraction clearly decreases with depth ( $R = -0.82$ ). The best-fit linear regression function is

$$S = -0.05 (D) + 164.52$$

where  $S$  = percent sand, and  $D$  = depth in meters. This simple model serves very well to predict grain-size distribution on this intermediate scale (Fig. 5).

In the eastern North Atlantic area, sampled from 1033 m to 5596 m, the model is once again inapplicable. There is a significant correlation between depth and percent sand ( $R = -0.57$ ), but the relationship may not be linear, and there is a much wider scatter of data. The value of  $R$  is probably inflated by the inclusion in the data of several deep samples with very low sand content. Since these samples lie below the calcite compensation depth (CCD) (Berger and Winterer, 1974), reduction of average grain size through dissolution is superimposed on the physical processes of sediment transport.

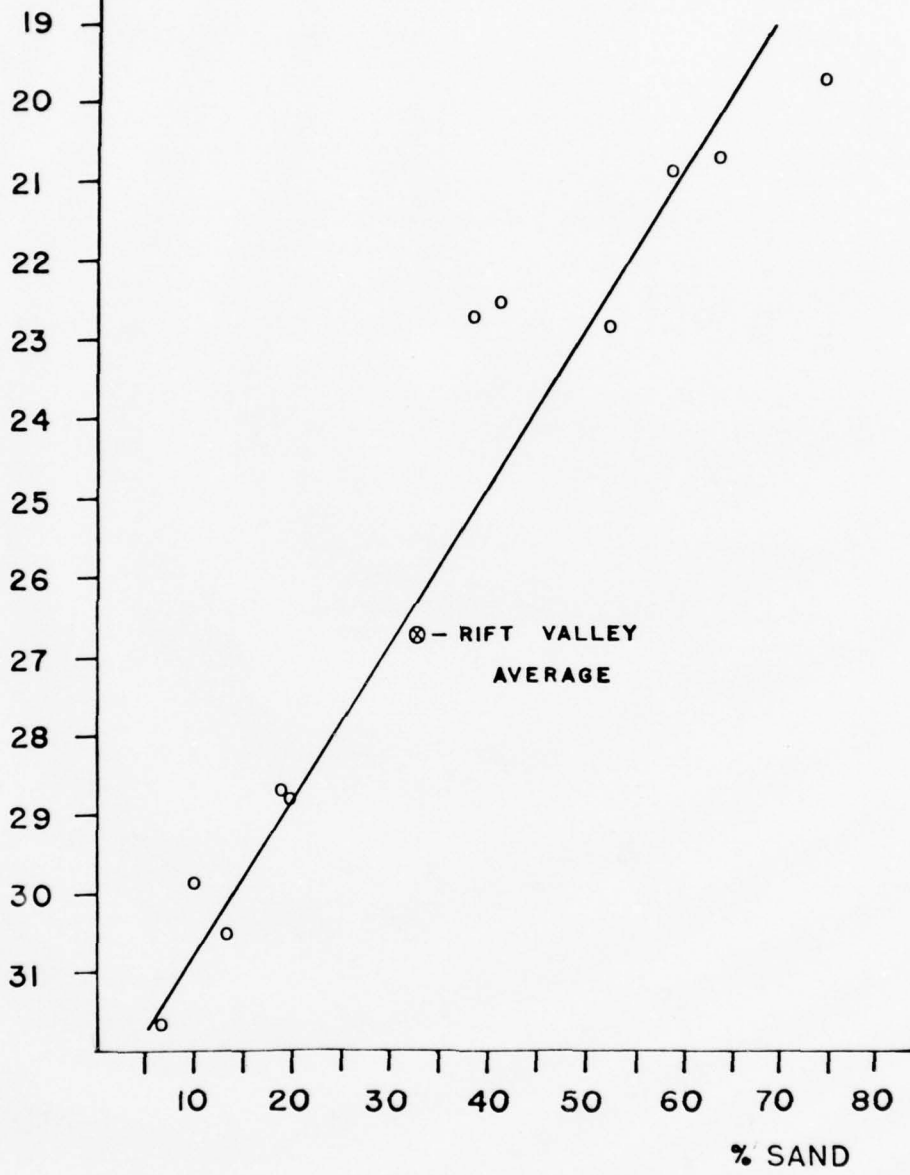
TABLE I

Correlation of sand percentage with depth of deposition. R is least squares correlation coefficient for depth versus percent sand-sized material.

Region	R
inner rift valley	-0.04
FAMOUS area	-0.82
eastern North Atlantic	-0.57

Figure 5. Relation of grain size to topography in FAMOUS area, showing linear decrease in coarse fraction (>63 microns) with increasing depth.

DEPTH  
M X 10<sup>2</sup>



The observed correlations between topography and grain size, in conjunction with evidence collected during submersible dives and from LIBEC photos, suggest that several mechanisms are responsible for sediment distribution patterns. The dominant trend appears to be transport of finer sediment fractions from relative topographic highs and redeposition in lower areas. The data above, which suggest this preferential movement of silt- and clay-sized material downslope, are abundantly supported by observations from Alvin.

It is clear from past work that redeposition of deep-sea sediments occurs on a regional scale (Ericson et al., 1955, 1961). Studies in the Panama Basin demonstrated that winnowing of finer material from ridge crests and redeposition in basin deeps, and lateral transport by tidal currents are important in determining sediment distribution patterns (Moore et al., 1973; van Andel, 1973). DSDP results from the eastern North Atlantic indicate that redeposition plays a major role in the initial formation of pelagic limestones and cherts (Berger and von Rad, 1972). A study of ponded sediments on the flanks of the Mid-Atlantic Ridge suggested that turbidity currents rebounding from valley walls are responsible for significant sediment transport (van Andel and Komar, 1969).

Inside the rift valley, however, there is no evidence that turbidity currents are significant in redepositing pelagic sediments (Tj.H. van Andel, personal communication), probably because too little sediment has accumulated as yet on the new crust. Instead, observations from Alvin indicate that bioturbation and gentle gravity transport of resuspended material continuously rework the sediments in association with bottom currents.

The importance of these relatively subtle, non-episodic processes of sediment redistribution has been postulated for abyssal hills regions by Berger and Piper (1972), who, however, considered mass slumping more important in areas of great relief. In the FAMOUS area, however, where slumping was seen especially on steeper slopes, the Alvin data strongly indicate that benthic stirring plays a much larger role than previously recognized.

The abundance and distribution of faunal trails and burrows indicate that the upper few centimeters of sediment are continually being reworked. Evidence for benthic faunal activity is widespread and varied. Observers noted tracks, trails, mounds, and burrows in large numbers throughout the inner rift valley (see Ballard and Moore, 1977, pp. 31, 103 for pictures of animal tracks). Commonly noted also were small avalanches which could easily be caused by organisms burrowing on sedimented slopes. Holothurians were frequently sighted, often in large groups, but in general the creatures responsible for stirring up the sediments were themselves not seen.

During the reworking process, some of the sediment is resuspended and becomes subject to downhill transport in that state. In a few cases, Alvin divers actually observed clouds of very fine suspended material lying immediately above the bottom and travelling very slowly down gentle slopes. Thus, the finer sediment fractions are carried in suspension by gravity for short distances before being redeposited at slightly greater depths. The grain-size data tend to support this model, which would likely result in differential redeposition, with

finer sediment fractions more easily resuspended, and thus transported further downslope.

This mechanism is minor compared to a mass slump or turbidity current, but the impact is large because it is a ubiquitous, long-term process. Although an undeniable contribution is made by sudden mass movements (for example, slope failure triggered by micro-earthquakes), it is important not to underestimate the long-term effects of redeposition through the more subtle agents of bioturbation.

In addition to a net downslope movement, this mechanism tends to partition the sediment into coarser and finer fractions, helping to explain the observed grain-size distribution. The gentle nature of transport accounts for the bias toward sandier, less readily suspended, material on high areas, since these sediments would have the longest residence time before being redeposited downslope.

Since gravitational redeposition is known to occur at many scales, the result (progressive fining of sediments with increasing depth) should be expressed at several scales. In the present study, grain-size data clearly define this relation at only one scale. This raises an important problem for deep-sea sediment studies in general, that of appropriate sample spacing for the area and processes under investigation.

For the eastern North Atlantic data, regional trends are somewhat visible, but the samples are too few and cover too large an area to display coherent patterns. Also, this set of data includes samples from below the CCD, which may modify linear patterns in grain-size trends.

Inside the rift valley, with relief varying tens of meters over distances of tens of meters, samples would have to be correspondingly closely-spaced in order to see the effects of small-scale transport processes. Furthermore, the vertical range is too limited (only about 200 m) to see the regional trend which becomes apparent only when the rift valley data are included with other FAMOUS area samples. If information from cores were not supplemented by detailed photo coverage and direct observation from Alvin, it would not be possible to document redeposition processes operating on the smallest scale within the valley. Submersible and photo evidence show that a striking range of physical and tectonic settings may occupy even a very small region of the sea floor. Accordingly, the sample spacing necessary to resolve details is of the order of meters.

#### Relations to currents inside the rift valley

Near-bottom currents in the inner rift valley are also responsible for some sediment redeposition. It has long been known that deep currents are strong enough to cause substantial movement of sediments (for example, Heezen and Hollister, 1964). More recently, they have been well documented at two sites in the rift valley, where they averaged 2.6 and 8.2 cm/sec (Keller et al., 1975). The flow within the valley is thought to depend heavily on tidal currents, locally influenced by topography.

Since currents are constrained within the walls of the valley, the predominant flow direction tends to parallel the north-northeast

(about  $022^{\circ}$ ) trend of the axis (Keller et al., 1975). On a regional scale, the expected result might be a thickening of sediments along this trend or higher concentrations of the finer sediments carried by the currents. Indeed, just beyond the ends of the rift valley, large sediment ponds have formed in the deeps at the junctures of rift valley segments and transforms (Tj.H. van Andel, personal communication).

No such patterns are observed inside the valley, for several possible reasons, including: 1) unidirectional flow to the northeast is observed only in the axial zone of the valley, whereas the flow consistently reverses along valley margins, under the influence of the semi-diurnal tides (Keller et al., 1975); 2) in the area of unidirectional flow, transport of sediments by currents is superimposed on the dominant trend of downslope movement discussed above, which apparently dictates regional distributions; 3) the irregular topography on the smallest scales results in numerous closed basins.

On the basis of observations from Alvin, however, there is ample evidence that bottom currents have a significant local effect on sediment transport. On many dives, observers noted ripple marks, generally about 2 to 5 cm high, with wavelengths of about 5 to 8 cm (Ballard and Moore, 1977, p. 61). There was no consistent orientation to these lineations throughout the rift valley, probably because of the effects of extreme topographic variability on local current direction. Observers also noted that ripples appear to be quickly obliterated by bioturbation, and so are transient phenomena whose absence does not necessarily indicate all absence of current activity.

More direct evidence for bottom currents was gleaned from the dives, with Alvin's current meters registering occasional speeds of several cm/sec. In addition, clouds of suspended sediment (sometimes generated by an Alvin touchdown) were often seen moving past the submersible while it was stationary.

On the smallest scale, currents have the most marked effect, frequently scouring small troughs beside individual basalt pillows. On one dive, observers noted depressions of this sort up to 30 cm deep around pillows.

#### Relations to rift axis

One additional trend in sediment size distribution is a progressive decrease in average grain size toward the rift axis. When data points are grouped according to distance from the volcanic axis, there is a distinct pattern (Table II). In light of possible associations with depth changes, projected sand percentages were calculated from the linear regression function presented above, using average depths of each group as the independent variable. The results strongly indicate that the observed trend is solely a function of depth (Table II).

#### Grain size modes

A more detailed textural analysis of the sediments was undertaken in the hope of further differentiating among distinct grain size categories. Following the methods discussed in detail by van Andel (1973), size frequency curves of sand and silt fractions of all sam-

TABLE II

Grain-size distribution in relation to rift axis.

Location of points	Avg. Depth	Avg. %			Predicted % Sand
		Sand	Silt	Clay	
outside rift valley	2335 m	46	18	36	48
inside rift valley					
>250 m from rift	2655 m	36	20	44	32
<250 m from rift	2645 m	28	22	50	32
virtually on axis (outside dive area)	3063 m	10	27	63	11

ples were analyzed using a DuPont 310 curve resolver at Oregon State University. The curve resolver permits the breakdown of the original size frequency distribution of a sample into modes, specifying their height, width, and position. The technique can be useful if major modes appear consistently in enough samples to determine patterns of distribution for an area. *How?*

For the sand fraction, five possible modes were recognized:

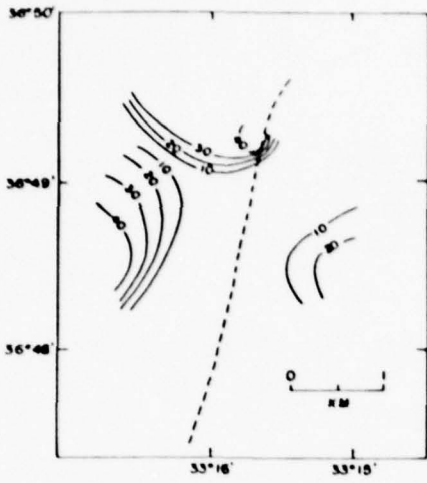
- A -- broad, minor mode centered at about 1.0 phi
- B -- distinct mode between 1.8 and 2.4 phi
- C -- less well-defined mode from 2.5 to 3.4 phi
- D -- distinct, narrow peak from 3.4 to 3.8 phi
- E -- major mode from 3.8 to 4.2 phi

When percentages of area under the frequency curve are mapped for each of these modes, the patterns are not very revealing (Fig. 6). Mode B appears to be concentrated in the eastern half of the rift valley, while Mode D is found primarily in one restricted area near the west wall. Modes A, C, and E are distributed irregularly throughout the valley, with no apparent relation to topography.

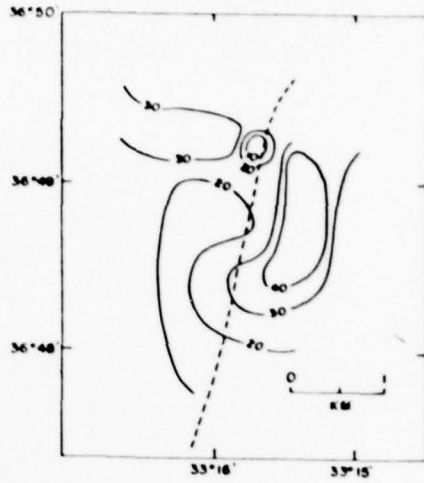
When samples within the rift valley are compared to those outside, some rift valley samples have a large contribution from Mode A, a mode virtually absent outside the rift valley, at both greater and lesser depths. It might be expected that this coarsest mode is composed of the larger volcanically-derived fragments of ash and glass associated with the rift axis, but its distribution within the valley does not support this idea (Fig. 6). On the other hand, a visual inspection of the samples near the valley margins in which this coarse

Figure 6. Distribution of sand modes A through E on inner rift valley floor. Contours mark the percent of the sand fraction represented by each mode. Dashed line shows position of rift axis.

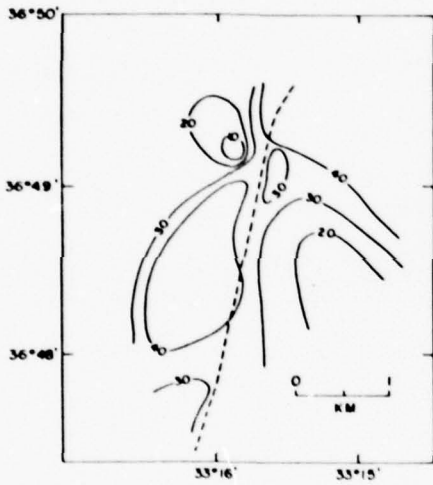
SAND MODE A



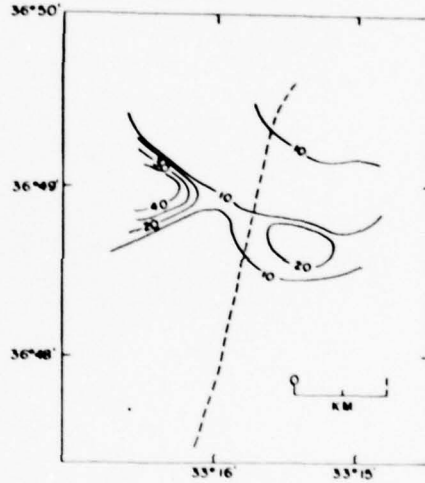
SAND MODE B



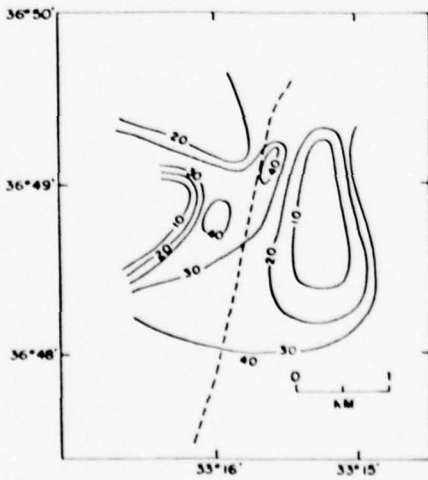
SAND MODE C



SAND MODE D



SAND MODE E



material is the dominant mode revealed a high concentration of tiny basalt fragments, probably broken off from talus piles near the walls. It seems likely, then, that Mode A actually comprises two unrelated classes of material: volcanic ash (concentrated near Mt. Venus) and fine basalt rubble (found primarily at the base of the steep west wall). The finer modes, on the other hand, are mainly composed of small individuals or fragments of foraminifera species making up coarser modes.

The silt fraction contains, in most samples, two basic size components: a major peak centered around 7.3 phi and a broad, minor "mode" around 5.3 phi. The ratio of the areas under the two peaks (fine/coarse) appears to be dependent to some degree on depth. For the entire FAMOUS area, the correlation coefficient for depth vs. this ratio is  $R = 0.53$ . (For FAMOUS-area samples outside the rift valley, plus one average value for inside the valley,  $R = 0.79$ ). This means that the finer component is found preferentially at greater depths, and that the components of the silt fraction follow the already-established regional patterns of sediment distribution. Within the rift valley,  $R = -0.31$ , but, as was demonstrated earlier, the sample spacing may lead to misleading conclusions about small-scale processes.

In summary, then, while a detailed textural analysis yields a few interesting observations, it is probably not well-suited to this region, which is very different from the marginal basins where it has been successfully employed in the past (van Andel, 1973; Thiede, 1977).

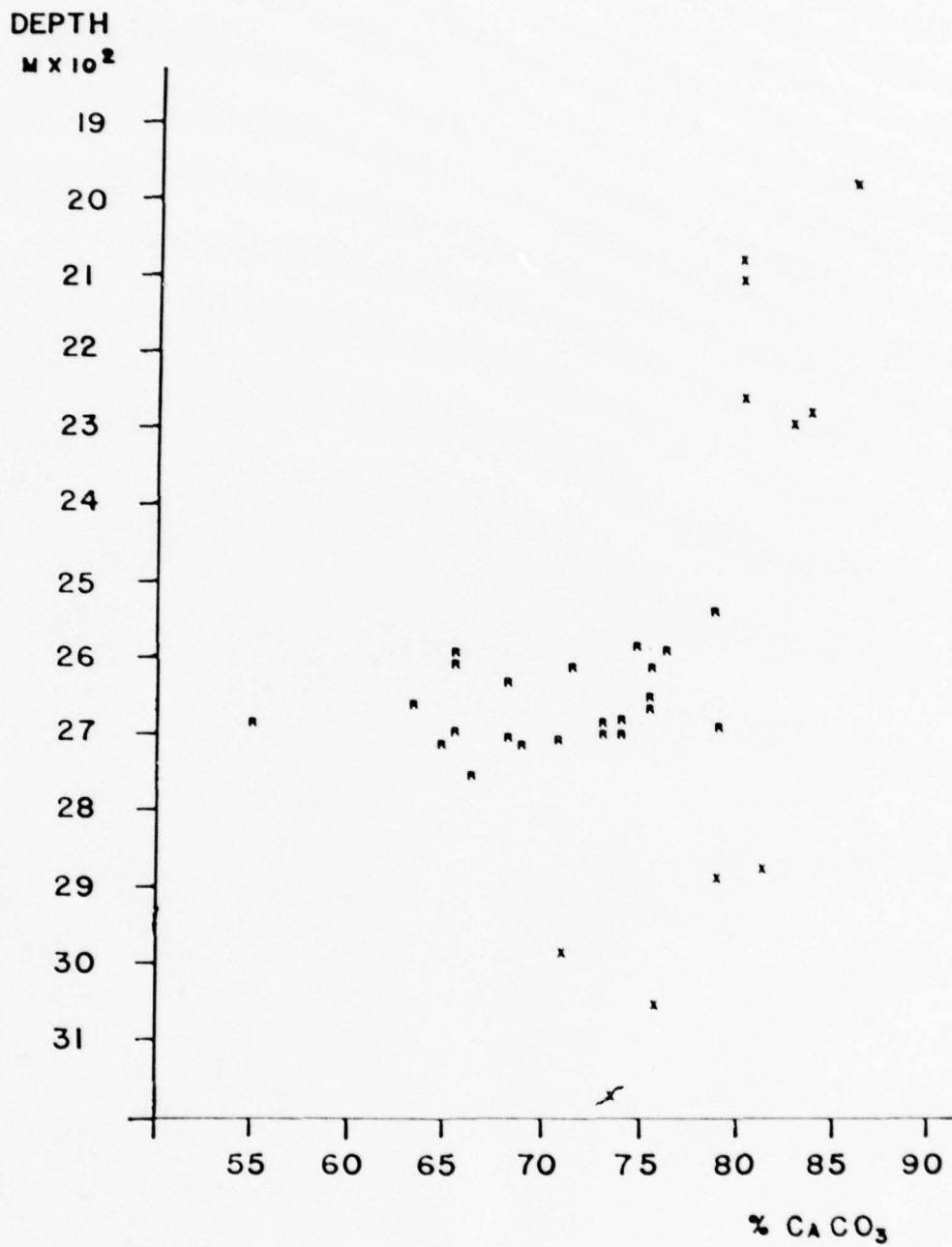
CaCO<sub>3</sub> CONTENT OF SEDIMENTS

The CaCO<sub>3</sub> content of the sediments was examined at the same three scales as grain-size patterns to determine any regional trends. Within the rift valley, no correlations were evident between CaCO<sub>3</sub> content and depth, distance from the rift axis, grain size, or depth in the core up to 1 m. Furthermore, in the entire FAMOUS area, CaCO<sub>3</sub> content is fairly constant (around 80-85%), with a slight decrease (to 70-75%) below 3000 m. The samples from the rift valley, which are at an intermediate depth for the area, are as a group anomalously low in CaCO<sub>3</sub>, averaging about 15% lower than the other sediments in the FAMOUS area (Fig. 7). Finally, in the eastern North Atlantic cores, CaCO<sub>3</sub> content averages about 80-85% down to about 4500 m. Below this depth, values decrease sharply, to near zero below 5400 m.

The decreasing values in the deeper sediments are expected, because the CCD in the central Atlantic lies near 5000 m (Berger and von Rad, 1972). In the intermediate-depth rift valley samples, however, the low CaCO<sub>3</sub> content is obviously not a result of approaching the CCD. The two most likely explanations are 1) accelerated dissolution of calcareous material as a result of chemical changes induced by volcanic activity, or 2) physical dilution of calcareous sediments by non-calcareous volcanic components.

The first explanation implies that the addition of volcanic gases would change the alkalinity of the water, and dissolve more CaCO<sub>3</sub>. There is no supporting evidence for this, and the coarser sediment

Figure 7. Relation of  $\text{CaCO}_3$  content to depth. Note anomalously low values for inner rift valley sediments (R), when compared to other FAMOUS area samples (X).



fractions show no signs of dissolution. This suggests that increased dissolution, if it occurs, does not play a major role.

The dilution of calcareous sediments by volcanic debris is easily confirmed by examining the coarse fraction. All sediments studied from the rift valley contain some volcanic material, principally large fragments of ash. However, substantially higher concentrations of volcanic debris in the sand fraction, observed in the vicinity of the rift axis, are not in conjunction with low  $\text{CaCO}_3$  values.

Possibly, a substantial amount of the volcanically-derived material is clay-sized and cannot be detected visually. If this were true, one would expect that rift valley sediments would have a larger clay-size fraction than sediments outside the area at comparable depths. The calculated average values for the clay-size fraction are 46% for sediments inside the rift valley, and 36% for sediments in the same depth range away from the rift valley. Since the two regions are presumably receiving similar pelagic influx, and topographic effects are minimized, the 10% difference may represent volcanic material produced inside the rift valley. This increase in non-calcareous sediment, which is fine enough to be transported throughout the valley, could easily account for the lower  $\text{CaCO}_3$  values.

## BENTHIC FORAMINIFERA

The use of benthic foraminifera in local environmental studies is usually confined to continental margins. For these areas, depth, temperature, and salinity relations are clearly established. In the deep ocean, benthic foraminiferal assemblages tend to be obscured in planktonic-rich sediments, and are therefore more difficult to study.

The sediments from the FAMOUS area present a unique opportunity to examine faunal distributions on a small scale. Representative benthic foraminiferal populations were extracted from the largely planktonic assemblages, in an effort to examine distributions in an area which is dramatically different from most of the ocean floor. Samples were selected from a traverse across the FAMOUS region, in order to determine how local variations reflect an environment which is geologically active, and thus highly changeable over both short times and short distances.

With pelagic sediments accumulating at a rate approximating  $3 \text{ cm}/10^3 \text{ yr}$  (Nozaki et al., 1977) and extensive and constant bioturbation, the benthic foraminiferal populations are highly diluted by planktonic material. In addition, admixing of older assemblages up into younger by organisms is fairly complete for the upper few centimeters of sediment (Berger and Heath, 1968). A time-dependent mixing model predicts a mixing rate,  $D$ , of  $10^2\text{-}10^3 \text{ cm}^2/10^3 \text{ yr}$  for surficial deep-sea sediments (Guinasso and Schink, 1975).

The analysis of one undisturbed core in the rift valley showed an 8-cm-deep mixed layer with nearly constant  $^{14}\text{C}$  dates of 2400 yr. The mixing rate was calculated to be  $189 \text{ cm}^2/10^3 \text{ yr}$ . A nearby core which had been physically disrupted had an age range from 13,000 yr at the top to about 18,000 yr at 15-17 cm depth (Nozaki et al., 1977). Clearly, then, the samples used for the present study contain mixed assemblages reflecting several thousand years of history. Unless there have been significant shifts in environment (for example, increased episodes of volcanism), for which there is no evidence, this uncertainty appears unimportant.

Ten samples were selected for determining benthic foraminiferal populations: six from the floor of the inner rift valley (Fig. 8), two from areas along adjacent fracture zones shallower than the rift, and two in the fracture zones in water deeper than the rift valley (Fig. 9). In all cases, the fraction larger than 63 microns was examined, except for station 31-118, where a sand fraction larger than 149 microns was available. Because most specimens observed in all samples were in the range larger than 149 microns anyway, this discrepancy should have little effect on results.

The sediments are composed largely of planktonic foraminifera; the benthic populations generally comprise less than 1%. In a study where hundreds of foraminifera might be examined without yielding a single benthic individual, a strictly quantitative approach was deemed impractical. For each sample, approximately 1200 ( $\pm 200$ ) foraminifera were looked at, and all specimens of benthic species were removed; generally only 20-30 benthic specimens were found in each sample.

Figure 8. Position of rift valley samples used in benthic foraminifera study. Field numbers are: 1)529-2/3, 2)519-1, 3)529-4, 4)529-5, 5)518-1, 6)526-4.

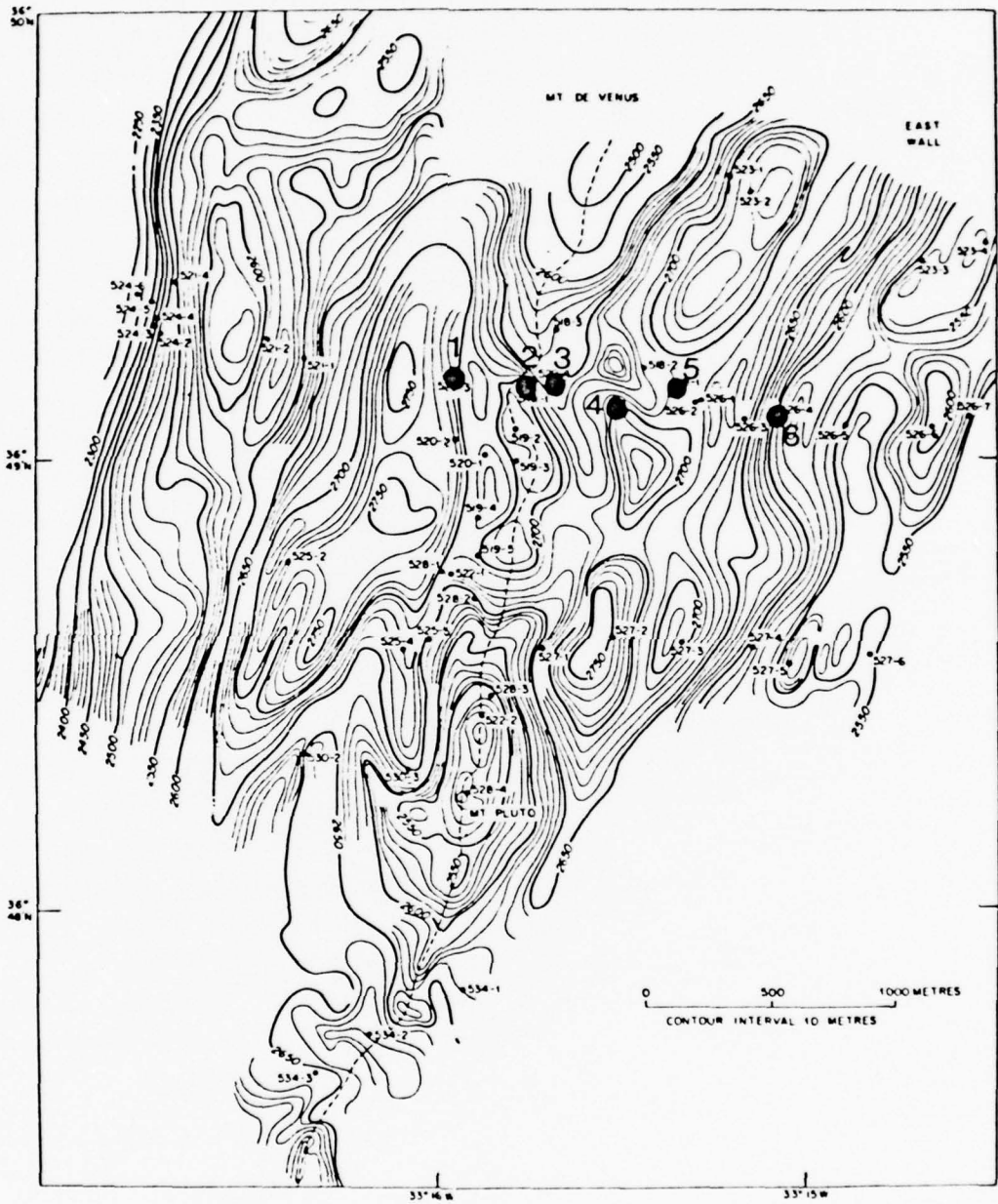
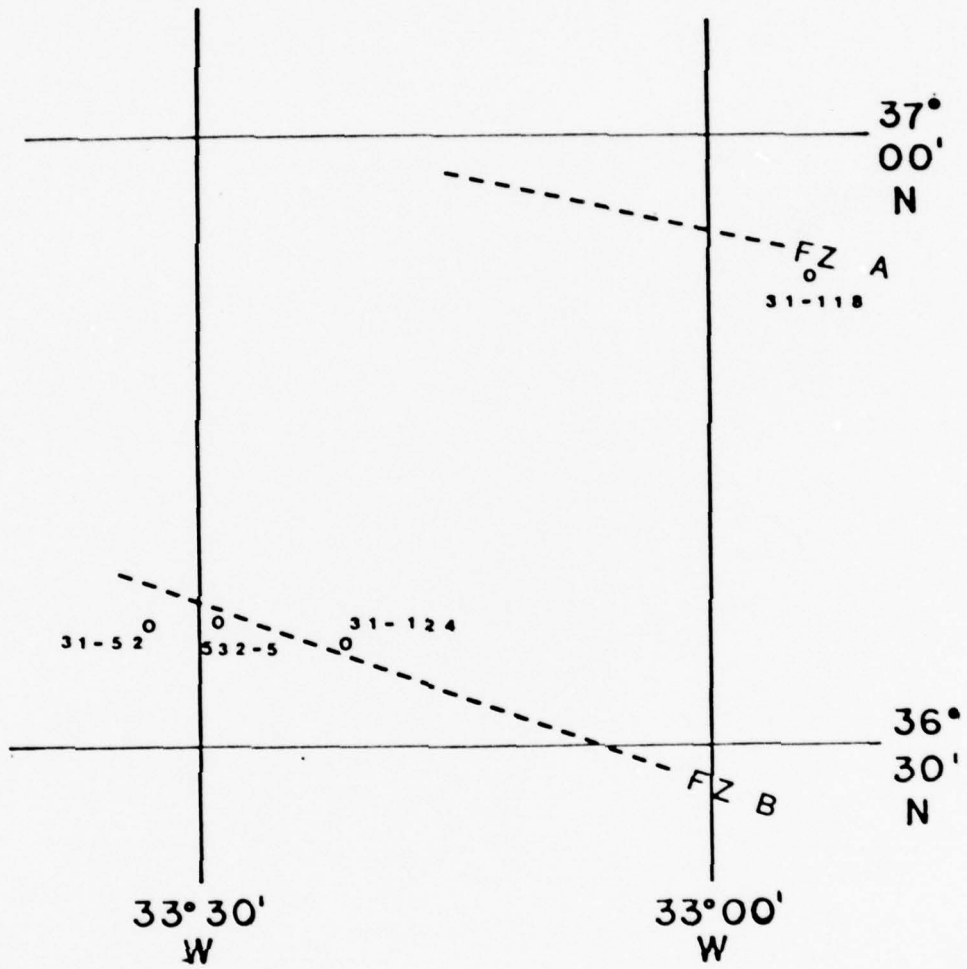


Figure 9. Position of samples associated with Fracture Zones A and B, used in foraminifera study.



These were identified to genus or species level with the help of Bandy and Rodolfo (1964), Barker (1960), Cushman (1931), Douglas (1973), Parker (1964), and J.C. Ingle (personal communication).

The results are somewhat limited because: 1) some samples are so small (e.g., 529-2/3) as to yield a minute benthic population, which cannot adequately represent numbers or diversity; 2) even in larger samples, benthic populations tend to be very small and erratically distributed within the sample; 3) biases result from differences in mean grain size due to selective transport. The samples with the coarsest sand fractions yielded the highest abundance and diversity, partly because benthic foraminifera tend to be among the larger individuals in a dominantly planktonic assemblage, and partly because larger foraminifera are much easier to sort and recognize. The genera observed, however, tend to overlap convincingly in all samples, irrespective of grain size, suggesting that size may be of minimal importance.

Given these limitations, the data show some surprisingly striking patterns in types and numbers of genera present. Brief station summaries may be found in the Appendix.

There are some general differences among the benthic foraminiferal assemblages of each of the three major provinces examined (Table III). One striking fact is the predominance of Planulina wuellerstorfi (Schwager) in samples taken from the shallower areas of the fracture zones. At station 532-5, this one species comprises nearly half of all benthics found, while at station 31-118, where there is considerably higher diversity, it still comprises over 20% of the



assemblage. Numbers of Planulina drop off sharply in both rift valley and deeper fracture zone regions, but still amount to 10% of a given assemblage. This decline might be a function of a parameter varying directly with depth (e.g., temperature, pressure, nutrients), with optimal conditions perhaps peaking around 2000 m. Alternately, as may be the case with some of these samples, the difference could be a local effect, for example, a temperature anomaly.

The abundance of Planulina in the shallow fracture zone sediments is coupled with relatively low percentages of porcelaneous and agglutinated foraminifera (Table IV). Agglutinated foraminifera in particular might be expected to increase in relative abundance with increasing depth as dissolution increases. Below 2000 m, however, no such trend is apparent; the percentages oscillate widely around the 10% level. Similar results were reported from the Peru-Chile trench, where Bandy and Rodolfo (1964) noted that, while calcareous forms clearly predominated down to 2000 m, calcareous-arenaceous ratios fluctuated wildly at greater depths. Even at 3000 m, the sediments in the FAMOUS area are sufficiently above the CCD to minimize the effects of dissolution. This is corroborated by the observation that the non-agglutinated benthic foraminifera present are fresh and lustrous even in the deepest sediments.

Perhaps the most intriguing trends are presented by smaller scale patterns and anomalies evidenced by the data. The two most striking are the miliolid distribution within the rift valley and concentrations of Rupertia stabilis (Wallich) at the Fracture Zone A site (31-118).

TABLE IV

Relative percentages of porcelaneous, calcareous hyaline, and agglutinated foraminifera.

Sample	Depth	Total #	%Porc.	%Calc.	%Aggl.
532-5	2061 m	25	20	80	0
31-118	2090 m	58	24	72	3
526-4	2585 m	29	34	59	7
529-4	2649 m	19	53	26	21
518-1	2690 m	30	43	53	3
529-5	2697 m	24	46	42	13
519-1	2705 m	36	50	44	6
529-2/3	2705 m	9	44	23	33
31-52	2878 m	30	33	53	13
31-124	2984 m	23	48	48	4

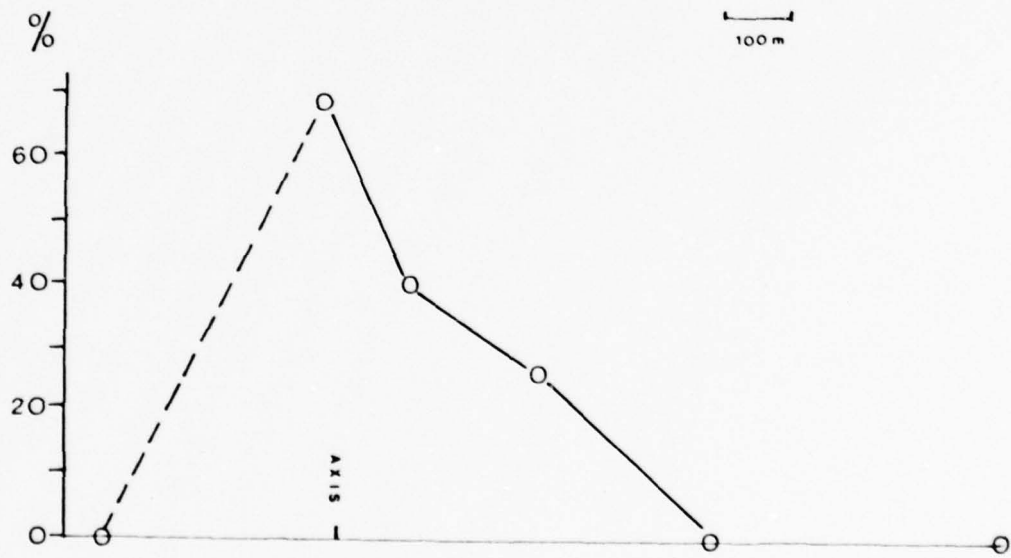
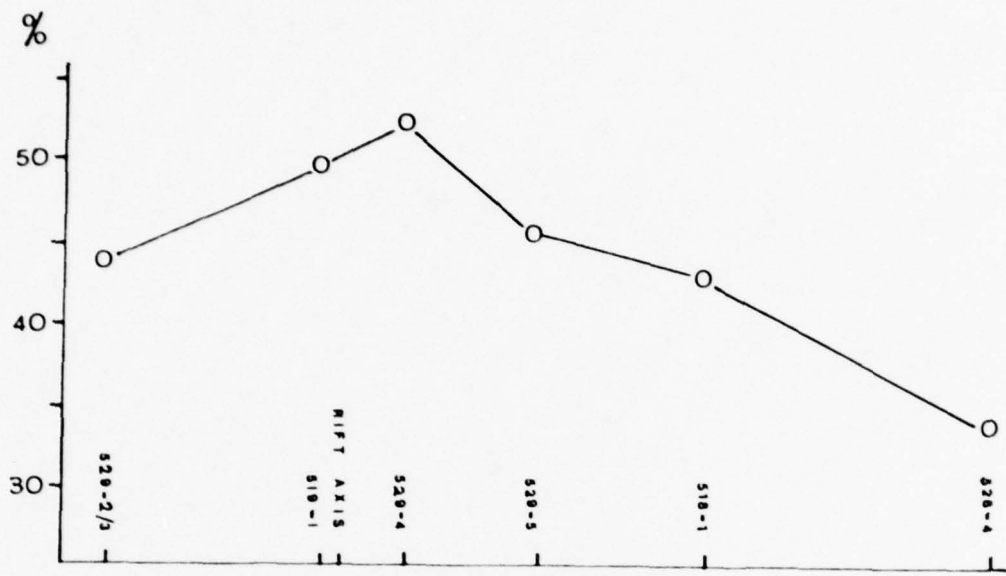
Within the rift valley, there is a clear relationship between relative percentages of porcelaneous foraminifera and distance from the rift axis (Fig. 10, top); numbers peak near the rift and fall off to either side. It is not known what process controls this association with proximity to a volcanic axis.

The more interesting aspect of this trend is the change in Spiroloculina abundance. This genus appears in only three of the rift valley samples, but in greatly differing proportions (Fig. 10, bottom). At the station nearest the rift axis (probably within tens of meters, the limits of navigational resolution), Spiroloculina accounts for 33% of the total assemblage and 67% of all porcelaneous forms. In the second closest station, the genus makes up 22% of the total and 40% of porcelaneous forms, and at the third site it comprises 13% of the total and 27% of porcelaneous forms. Beyond about 300 m from the rift axis, no further instances of Spiroloculina were noted in this set of samples, although one specimen was recovered from sample 532-5.

This puzzling distribution is a more dramatic example of the type of pattern displayed by porcelaneous foraminifera as a group. Spiroloculina may be particularly sensitive to variations in temperature, pH, concentrations of certain gases (e.g., CO<sub>2</sub>), substrate composition, or any other combination of factors which could be associated with volcanic processes. Further work is needed to determine a more precise distribution of Spiroloculina, both in relation to the rift zone and to subtle variations in physical parameters.

Figure 10. Top: Distribution of porcelaneous foraminifera across rift axis. Vertical axis shows percent porcelaneous individuals in the benthic assemblage. Horizontal: sample position along traverse of Figure 8.

Bottom: Distribution of Spiroloculina across rift axis. Vertical axis shows percent of this genus in the porcelaneous assemblage.



A second notable anomaly is the occurrence of Rupertia stabilis at site 31-118, along Fracture Zone A. Although absent in all other samples, Rupertia accounts for fully 14% of the benthic foraminifera at this one station. Rupertia is an uncommon attached form which is most often encountered in relatively warm, highly productive waters near continental margins (J.C. Ingle and Tj.H. van Andel, personal communication). One hypothesis which could relate this type of environment to the site at which Rupertia was found is the possible presence of hydrothermal vents with associated abundant fauna, as observed on the Galapagos rift (Corliss et al., 1979). Such vents create local effects of anomalously warm water and high productivity which might favor the proliferation of Rupertia. In addition, it could help explain the relatively high diversity of benthic foraminifera at this site, which is the highest of all locations sampled.

Water temperature profiles taken in the FAMOUS area indicate that the entire rift valley has bottom water temperatures about 1° C above normal for that depth, and that there are also variations along the fracture zones. Temperatures observed below 2200 m increase from 3.53° C in the western part of Fracture Zone B to 3.80° C in the eastern part of Fracture Zone A, which is close to station 31-118 (Fehn et al., 1977). Although these temperature anomalies can be largely explained by hydrodynamic effects, the same study admits the possibility that hydrothermal plumes may cause local anomalies.

The results of a heat flow study strongly indicate the presence of a hydrothermal circulation system in the Fracture Zone A area

(Williams et al., 1977). Two inactive hydrothermal vents observed in the region are believed to have been active in the very recent past (Arcyana, 1975). Although the evidence is inconclusive, the presence of Rupertia tends to further support a hydrothermal circulation model for Fracture Zone A, perhaps including active vents that have not yet been discovered.

A great deal more work is required before clear associations can be drawn between local benthic populations and subtle environmental variations. What the results of the present study do demonstrate is the surprising variability of benthic foraminiferal assemblages over a very small portion of the sea floor.

## CONCLUSIONS

1. Sediment cover on the floor of the inner rift valley is roughly a function of age of the underlying crust and reflects asymmetric spreading. This pattern is modified by redeposition of sediments in topographic depressions adjacent to volcanic highs.

2. Grain size is highly correlated with depth over the whole FAMOUS area. The relation can be described by a simple linear function, with progressively finer sediments found at greater depth.

3. Extensive bioturbation, leading to resuspension of fine material and gentle gravity transport, appears to be the most significant long-term agent of redeposition. Episodic processes, such as slumping, are believed to be less important to observed grain-size distribution patterns.

4. Although downhill transport is known to occur at all scales, it is clearly shown in the grain-size data at only the intermediate of the three scales studied. In particular, the relation of sample spacing to relief scale masks any correlations between depth and grain size within the inner rift valley, even for the smallest-scale data set.

5. The primary effect of currents in the inner rift valley is localized; they form many transient ripple and scour features at a scale of a few centimeters.

6. An apparent decrease in grain size with increasing proximity to the rift axis is found to be a function of depth alone.

7. Detailed textural analyses of rift valley sediments do not reveal any new patterns. The five inferred sand modes are irregularly distributed and probably do not represent distinct sediment components. A bimodal silt fraction appears to follow more general grain-size trends.

8.  $\text{CaCO}_3$  content is anomalously low in sediments of the inner rift valley, when compared to surrounding sediments of comparable depth. Dilution of calcareous sediments by volcanically-derived components is probably responsible for the lower values. High content of clay-sized material in rift valley sediments suggests that much of the volcanic material may be very fine-grained.

9. Benthic foraminifera populations in the FAMOUS area are surprisingly variable over very short distances. Unusual distributions of porcelaneous forms appear to be related to the position of the volcanic axis. A highly localized concentration of Rupertia near Fracture Zone A may possibly reflect recent hydrothermal activity.

## REFERENCES

- ARCYANA, 1975. Transform fault and rift valley from bathyscaph and diving saucer. *Science*, 190: 108-116.
- Ballard, R.D., and Moore, J.G., 1977. Photographic atlas of the Mid-Atlantic Ridge rift valley. Springer-Verlag, New York, 114 pp.
- Ballard, R.D., and van Andel, Tj., 1977a. Project FAMOUS: Operational techniques and American submersible operations. *Geol. Soc. America Bull.*, 88: 495-506.
- Ballard, R.D., and van Andel, Tj., 1977b. Morphology and tectonics of the inner rift valley at lat 36°50' N on the Mid-Atlantic Ridge. *Geol. Soc. America Bull.*, 88: 507-530.
- Bandy, O.L., and Rodolfo, K.S., 1964. Distribution of foraminifera and sediments; Peru-Chile Trench area. *Deep Sea Research*, 11: 817-837.
- Barker, R.W., 1960. Taxonomic notes on species figured by H.B. Brady in his report on the foraminifera dredged by H.M.S. Challenger during years 1873-1876. *Soc. Econ. Paleontol. Mineral., Spec. Publ.* 9, 238 pp.
- Berger, W.H., and Heath, G.R., 1968. Vertical mixing in pelagic sediments. *Sears Foundation: Jour. Marine Research*, 26(2), 124-143.
- Berger, W.H., and Piper, D.J.W., 1972. Planktonic foraminifera; differential settling, dissolution, and redeposition. *Limnol. Oceanogr.*, 17: 275-287.
- Berger, W.H., and von Rad, U., 1972. Cretaceous and Cenozoic sediments from the Atlantic Ocean. In: *Initial Reports of the Deep Sea Drilling Project, XIV*, U.S. Govt. Printing Office, Washington: 787-954.
- Berger, W.H., and Winterer, E.L., 1974. Plate stratigraphy and the fluctuating carbonate line. In: K.J. Hsu and H.C. Jenkyns (Editors), *Pelagic sediments on land and in the sea*. *Intl. Assoc. Sediment. spec. pub.* 1: 11-48.
- Bryan, W.B., and Moore, J.G., 1977. Compositional variations of young basalts in the Mid-Atlantic Ridge rift valley near 36°49'N. *Geol. Soc. America Bull.*, 88: 556-570.

- Brundage, W.L., and Cherkis, N.Z., 1975. Preliminary LIBEC/FAMOUS cruise results. U.S. Naval Research Lab. Rept. 7785: 31 pp.
- Corliss, J.B., Dymond, J., Gordon, L.I., Edmond, J.M., Von Herzen, R.P., Ballard, R.D., Green, K., Williams, D.L., Bainbridge, A., Crane, K., and van Andel, Tj.H., 1979. Submarine thermal springs on the Galapagos Rift. *Science*, in press.
- Cushman, J.A., 1931. The foraminifera of the Atlantic Ocean. U.S. National Museum Bull., 104, Parts 1-8 (1918-1931).
- Douglas, R.G., 1973. Benthonic foraminiferal biostratigraphy in the central North Pacific, Leg 17, Deep Sea Drilling Project. In: Initial Reports of the Deep Sea Drilling Project, XVII, 607-671.
- Ericson, D.B., Ewing, M., Heezen, B.C., and Wollin, G., 1955. Sediment deposition in deep Atlantic. *Geol. Soc. America Spec. Paper*, 62: 205-220.
- Ericson, D.B., Ewing, M., Wollin, G., and Heezen, B.C., 1961. Atlantic deep-sea sediment cores. *Geol. Soc. America Bull.*, 72: 193-286.
- Fehn, U., Robinson, G.R., Siegel, M.D., Williams, D.L., Erickson, A.J., and Holland, H.D., 1977. Water temperature in the FAMOUS area. *Geol. Soc. America Bull.*, 88: 488-494.
- Guinasso, N.L., and Schink, D.R., 1975. Quantitative estimates of biological mixing rates in abyssal sediments. *Jour. Geophys. Research*, 80: 3032-3043.
- Heezen, B.C., and Hollister, C.D., 1964. Deep-sea current evidence from abyssal sediments. *Marine Geol.*, 1: 141-174.
- Heirtzler, J.R., and van Andel, Tj., 1977. Project FAMOUS: its origin, programs, and setting. *Geol. Soc. America Bull.*, 88: 481-487.
- Keller, G.H., Anderson, S.H., and Lavelle, J.W., 1975. Near-bottom currents in the Mid-Atlantic Ridge rift valley. *Canad. Jour. Earth Sci.*, 12: 703-710.
- Macdonald, K.C., Luyendyk, B.P., Mudie, J.D., and Spiess, F.N., 1975. Near-bottom geophysical study of the Mid-Atlantic Ridge median valley near lat 37° N: Preliminary observations. *Geology*, 13: 211-215.
- Moore, T.C., Jr., Heath, G.R., and Kowsmann, R.O., 1973. Biogenic sediments of the Panama Basin. *Jour. Geol.*, 81: 458-472.

- Nozaki, Y., Cochran, J.K., Turekian, K.K., and Keller, G.H., 1977. Radiocarbon and  $^{210}\text{Pb}$  distribution in submersible-taken deep-sea cores from Project FAMOUS. *Earth Plan. Sci. Letters*, 34: 167-173.
- Parker, F.L., 1964. Foraminifera from the experimental Mohole drilling near Guadalupe Island, Mexico. *Jour. Paleontol.*, 38: 617-637.
- Ramberg, I.B., and van Andel, Tj., 1977. Morphology and tectonic evolution of the rift valley at lat  $36^{\circ}30'$  N, Mid-Atlantic Ridge. *Geol. Soc. America Bull.*, 88: 577-586.
- Thiede, J., 1977. Textural variations of calcareous coarse fractions in the Panama Basin (eastern equatorial Pacific Ocean). In: N.R. Andersen and A. Malahoff (Editors), *The fate of fossil fuel  $\text{CO}_2$  in the oceans*, Plenum Pub. Corp., New York: 673-692.
- Thiede, J., Chriss, T., Clauson, M., and Swift, S.A., 1976. Settling tubes for size analysis of fine and coarse fractions of oceanic sediments. *Tech. Rep.*, 76-8, School Oceanogr., Oregon State Univ., Corvallis: 87 pp.
- van Andel, Tj., 1973, Texture and dispersal of sediments in the Panama Basin. *Jour. Geol.*, 81: 434-457.
- van Andel, Tj., and Komar, P.D., 1969. Pondered sediments of the mid-Atlantic Ridge between  $22^{\circ}$  and  $23^{\circ}$  North latitude. *Geol. Soc. America Bull.*, 80: 1163-1190.
- Williams, D.L., Lee, T., Von Herzen, R.P., Green, K.E., and Hobart, M.A., 1977. A geothermal study of the Mid-Atlantic Ridge near  $37^{\circ}$  N. *Geol. Soc. America Bull.*, 88: 531-540.

## APPENDIX: BENTHIC FORAMINIFERA STATION SUMMARIES

Station 532-5, 2061 m

1 Pyrgo  
 1 Quinqueloculina  
 1 Spiroloculina  
 2 broken/unidentified miliolids

---

5 porcelaneous forms

1 Fissurina  
 2 Gyroidina sp. A (fat, opaque test, sutures indistinct)  
 1 Gyroidina sp. B (less robust, translucent test, sutures distinct)  
 1 Melonis pomplioides (Fichtel and Moll)  
 1 Nodosaria antillea (Cushman)  
 11 Planulina wuellerstorfi (Schwager)  
 1 Uvigerina peregrina aff. (Cushman)  
 1 Uvigerina sp.  
 1 unidentified rotalid

---

20 calcareous hyaline forms

0 agglutinated forms

25 total

Sample description:

Location: Fracture Zone B

Mean grain size: medium to coarse sand

Notes: little to no volcanic debris, very clean, mostly planktonic foraminifera with few other forms present.

Station 31-118, 2090 m

4 Pyrgo  
 1 Triloculina  
 9 broken/unidentified miliolids

---

14 porcelaneous forms

1 *Bulimina inflata* aff. (Seguenza)  
 1 *Cassidulina subglobosa* (Brady) var. *quadrata* (Cushman and Hughes)  
 6 *Cibicidoides kullenbergi* (Parker)  
 1 *Ehrenbergina pacifica* aff. (Cushman)  
 1 *Gyroidina* sp. A  
 6 *Hoeglundina elegans* (d'Orbigny)  
 2 *Laticarinina pauperata* (Parker and Jones)  
 1 *Melonis pomplioides* (Fichtel and Moll)  
 13 *Planulina wuellerstorfi* (Schwager)  
 1 *Pullenia subcarinata* (d'Orbigny)  
 8 *Rupertia stabilis* (Wallich)  
 1 unidentified rotalid

---

42 calcareous hyaline forms

1 Bathysiphon  
 1 unidentified agglutinated

---

2 agglutinated forms

58 total

Sample description:

Location: Fracture Zone A

Mean Grain Size: medium to coarse sand

Notes: little to no volcanic debris; very clean, mostly planktonic foraminifera with few other forms present

Station 526-4, 2585 m.

4 Pyrgo  
 2 Quinqueloculina  
 1 Sigmoidopsis  
 3 broken/unidentified miliolids

---

10 porcelaneous forms

2 Cibicidoides kullenbergi (Parker)  
 3 Fissurina  
 5 Hoeglundina elegans (d'Orbigny)  
 1 Laticarinina pauperata (Parker and Jones)  
 1 Oolina sp. A (transparent, costate)  
 1 Oolina sp. B (transparent, unornamented)  
 4 Planulina wuellerstorfi (Schwager)

---

17 calcareous hyaline forms

1 Bathysiphon  
 1 Karreriella bradyi (Cushman)

---

2 agglutinated forms

29 total

Sample description:

Location: rift valley, 975 m east of axis

Mean grain size: medium sand

Notes: mostly planktonic foraminifera with some volcanic ash,  
 Mn-coated fragments, more pteropods, echinoderm spines,  
 sponge spicules, radiolaria, etc.

Station 529-4, 2649 m

2 Quinqueloculina  
4 Spiroloculina  
4 broken/unidentified miliolids

---

10 porcelaneous forms

1 Cibicides sp.  
1 Fissurina  
1 Planulina wuellerstorfi (Schwager)  
1 Spirillina  
1 Uvigerina peregrina aff. (Cushman)

---

5 calcareous hyaline forms

1 Ammodiscus  
1 Bathysiphon  
2 Karreriella bradyi (Cushman)

---

4 agglutinated forms

19 total

Sample description:

Location: rift valley, 100 m east of axis

Mean grain size: medium sand

Notes: mostly planktonic foraminifera, considerable volcanic debris, including ash and glass shards; some sponge spicules, radiolaria, etc.

Station 518-1, 2690 m

2 Pyrgo  
2 Quinqueloculina  
9 broken/unidentified miliolids

---

13 porcelaneous forms

1 Cibicidoides kullenbergi (Parker)  
2 Fissurina  
5 Hoeglundina elegans (d'Orbigny)  
3 Laticarinina pauperata (Parker and Jones)  
2 Melonis pomplioides (Fichtel and Moll)  
3 Planulina wuellerstorfi (Schwager)

---

16 calcareous hyaline forms

1 Bathysiphon

---

1 agglutinated form

30 total

Sample description:

Location: rift valley, 550 m east of axis

Mean grain size: medium sand

Notes: mostly planktonic foraminifera, with common volcanic ash, Mn-coated fragments; sponge spicules.

Station 529-5, 2697 m

2 Quinqueloculina  
3 Spiroloculina  
6 broken/unidentified miliolids

---

11 porcelaneous forms

1 Cibicidoides kullenbergi (Parker)  
1 Fissurina  
2 Laticarinina pauperata (Parker and Jones)  
1 Melonis pomplioides (Fichtel and Moll)  
4 Planulina wuellerstorfi (Schwager)  
1 Planulina aff. sp. A

---

10 calcareous hyaline forms

2 Bathysiphon  
1 Karreriella bradyi (Cushman)

---

3 agglutinated forms

24 total

Sample description:

Location: rift valley, 300 m east of axis

Mean grain size: medium sand

Notes: mostly planktonic foraminifera with much volcanic ash,  
glass shard, Mn-coated fragments, plus sponge spicules.

Station 519-1, 2705 m

2 Quinqueloculina  
12 Spiroloculina  
4 broken/unidentified miliolids

---

18 porcelaneous forms

1 Gyroidina sp. C (very small, transparent test)  
6 Hoeglundina elegans (d'Orbigny)  
2 Laticarinina pauperata (Parker and Jones)  
1 Melonis pomplioides (Fichtel and Moll)  
1 Planulina aff. sp. A  
3 Planulina wuellerstorfi (Schwager)  
2 Pullenia subcarinata (d'Orbigny)

---

16 calcareous hyaline forms

1 Bathysiphon  
1 Karreriella bradyi (Cushman)

---

2 agglutinated forms

36 total

Sample description:

Location: rift valley, 25 m west of axis

Mean grain size: medium sand

Notes: planktonic foraminifera with large chunks of volcanic ash, glass, Mn-coated fragments, sponge spicules.

Station 529-2/3, 2705 m

3 Quinqueloculina  
1 broken/unidentified miliolid

---

4 porcelaneous forms

1 Bolivina sp. A (small, costate)  
1 Uvigerina peregrina aff. (Cushman)

---

2 calcareous hyaline forms

3 Bathysiphon

---

3 agglutinated forms

9 total

Sample description:

Location: rift valley, 350 m west of axis

Mean grain size: medium sand

Notes: very small sample, many large pieces of volcanic ash.

Station 31-52, 2878 m

2 Pyrgo  
4 Quinqueloculina  
4 broken/unidentified miliolids

---

10 porcelaneous forms

1 Bolivina sp. A  
2 Cibicidoides kullenbergi (Parker)  
1 Fissurina wiesneri (Barker)  
1 Gyroidina sp. B  
4 Hoeglundina elegans (d'Orbigny)  
4 Laticarinina pauperata (Parker and Jones)  
3 Planulina wuellerstorfi (Schwager)

---

16 calcareous hyaline forms

4 Bathysiphon

---

4 agglutinated forms

30 total

Sample description:

Location: Fracture Zone B

Mean grain size: fine to medium sand

Notes: virtually all planktonic foraminifera, extremely clean,  
free of volcanic debris and other organisms.

Station 31-124, 2984 m

3 Pyrgo  
3 Quinqueloculina  
5 broken/unidentified miliolids

---

11 porcelaneous forms

1 Bolivina sp. A  
1 Cibicidoides kullenbergi (Parker)  
1 Gyroidina sp. B  
1 Gyroidina sp. C  
1 Hoeglundina elegans (d'Orbigny)  
2 Laticarinina pauperata (Parker and Jones)  
1 Melonis pomplioides (Fichtel and Moll)  
2 Planulina wuellerstorfi (Schwager)  
1 Uvigerina peregrina aff. (Cushman)

---

11 calcareous hyaline forms

1 Bathysiphon  
1 Textularia abbreviata aff. (d'Orbigny)

---

2 agglutinated forms

23 total

Sample description:

Location: Fracture Zone B

Mean grain size: fine to medium sand

Notes: virtually all planktonic foraminifera, extremely clean,  
free of volcanic debris and other organisms.